Journal of Medicinal Chemistry

Article

Synthesis, Binding Affinity at Glutamic Acid Receptors, Neuroprotective Effects, and Molecular Modeling Investigation of Novel Dihydroisoxazole Amino Acids

Paola Conti, Marco De Amici, Giovanni Grazioso, Gabriella Roda, Andrea Pinto, Kasper B Hansen, Birgitte Nielsen, Ulf Madsen, Hans Bruner-Osborne, Jan Egebjerg, Valentina Vestri, Domenico E. Pellegrini-Giampietro, Pauline Sibille, Francine C. Acher, and Carlo De Micheli

J. Med. Chem., **2005**, 48 (20), 6315-6325• DOI: 10.1021/jm0504499 • Publication Date (Web): 13 September 2005

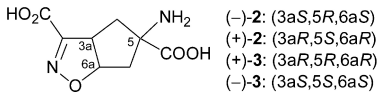

(–)-**2**: (3a*S*,5*R*,6a*S*)
(+)-**2**: (3a*R*,5*S*,6a*R*)
(+)-**3**: (3a*R*,5*R*,6a*R*)
(–)-**3**: (3a*S*,5*S*,6a*S*)

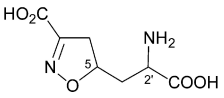

(+)-**4**: (5*R*,2'*S*)
(–)-**4**: (5*S*,2'*R*)
(+)-**5**: (5*R*,2'*R*)
(–)-**5**: (5*S*,2'*S*)

More About This Article

Additional resources and features associated with this article are available within the HTML version:

- Supporting Information
- Links to the 1 articles that cite this article, as of the time of this article download
- Access to high resolution figures
- Links to articles and content related to this article
- Copyright permission to reproduce figures and/or text from this article

View the Full Text HTML

Journal of Medicinal Chemistry is published by the American Chemical Society. 1155 Sixteenth Street N.W., Washington, DC 20036

Synthesis, Binding Affinity at Glutamic Acid Receptors, Neuroprotective Effects, and Molecular Modeling Investigation of Novel Dihydroisoxazole Amino Acids†

Paola Conti,‡ Marco De Amici,‡ Giovanni Grazioso,‡ Gabriella Roda,‡ Andrea Pinto,‡ Kasper Bø Hansen,§,# Birgitte Nielsen,§ Ulf Madsen,§ Hans Bräuner-Osborne,§ Jan Egebjerg,# Valentina Vestri,⊥ Domenico E. Pellegrini-Giampietro,⊥ Pauline Sibille,⊗ Francine C. Acher,⊗ and Carlo De Micheli‡,*

Istituto di Chimica Farmaceutica e Tossicologica, Università degli Studi di Milano, Viale Abruzzi 42, 20131 Milano, Italy; Department of Medicinal Chemistry, The Danish University of Pharmaceutical Sciences, Universitetsparken 2, DK-2500 Copenhagen, Denmark; Department of Molecular Biology, H. Lundbeck A/S, Valby, Denmark; Dipartimento di Farmacologia Preclinica e Clinica, Università degli Studi di Firenze, viale G. Pieraccini, 6, 50139 Firenze, Italy; and Laboratoire de Chimie et Biochimie Pharmacologiques et Toxicologiques, UMR8601-CNRS, Université René Descartes-Paris V, 45 rue des Saints-Pères, 75270 Paris Cedex 06, France

Received May 11, 2005

The four stereoisomers of 5-(2-amino-2-carboxyethyl)-4,5-dihydroisoxazole-3-carboxylic acid-(+)-**4**, (−)-**4**, (+)-**5**, and (−)-**5** were prepared by stereoselective synthesis of two pairs of enantiomers, which were subsequently resolved by enzymatic procedures. These four stereoisomers and the four stereoisomers of the bicyclic analogue 5-amino-4,5,6,6a-tetrahydro-3a*H*-cyclopenta[*d*]isoxazole-3,5-dicarboxylic acid (+)-**2,** (−)-**2**, (+)-**3**, and (−)-**3** were tested at ionotropic and metabotropic glutamate receptor subtypes. The most potent NMDA receptor antagonists [(+)-**2**, (−)-**4**, and (+)-**5**] showed a significant neuroprotective effect when tested in an oxygen glucose deprivation (OGD) cell culture test. The same compounds were preliminarily assayed using *Xenopus* oocytes expressing cloned rat NMDA receptors containing the NR1 subunit in combination with either NR2A, NR2B, NR2C, or NR2D subunit. In this assay, all three derivatives showed high antagonist potency with preference for the NR2A and NR2B subtypes, with derivative (−)-**4** behaving as the most potent antagonist. The biological data are discussed on the basis of homology models reported in the literature for NMDA receptors and mGluRs.

Introduction

The acidic amino acid glutamate (Glu), the major neurotransmitter of the fast excitatory synapses in the central nervous system (CNS), plays a pivotal role in physiological processes ranging from learning and memory to control of movements and pain sensitivity.[1,2] Glu induces toxicity (excitotoxicity) by an overflow into the synaptic cleft which can occur following metabolic disturbances, and similar excitotoxicity can be caused by overstimulation of Glu receptors by endogenous or exogenous substances.[1,2] Glu activity is mediated by ionotropic (iGluRs) and metabotropic Glu receptors (mGluRs).[3,4] The mGluRs exert modulatory effects on neuronal excitability and synaptic transmission. Up to now, eight mGluR subtypes and multiple splice variants have been cloned from mammalian brain.[4] They have been subdivided into three groups on the basis of their sequence homology, coupling mechanisms, and pharmacology. Group I (mGluR1,5) is positively coupled to phospholipase C (PLC) whereas group II (mGluR2,3) and group III (mGluR4,6,7,8) are coupled via Gi/o proteins to adenylyl cyclase inhibition.[4]

The iGluRs are associated with integral cation-specific ion channels and include the *N*-methyl-D-aspartate (NMDA), 2-amino-3-(5-methyl-3-hydroxyisoxazol-4-yl)-propanoic acid (AMPA), and kainate (KA) types.[3] Whereas the endogenous ligand for AMPA and KA receptors is Glu, activation of NMDA receptors require simultaneous binding of both Glu and glycine.[5] Since overstimulation of NMDA receptors produces acute neurodegeneration, much research has been focused on the development of selective antagonists as neuroprotective agents.

In the past decade, the molecular biology of the NMDA receptor family has been defined, and now we know that these receptors are tetramers composed of two NR1 subunits in combination with two NR2 subunits[6] or, less commonly, NR3 subunits.[7,8] Since nonselective NMDA receptor antagonists are characterized by a number of adverse CNS effects, including hallucinations, a centrally mediated increase in blood pressure and, at high doses, catatonia and anesthesia,[9,10] current interest largely centers on the development of potent and NR2B subtype-selective antagonists,[11,12] e.g. Ifenprodil **1** (Figure 1). In preclinical tests these compounds appear to lack the side-effects commonly associated with nonselective NMDA receptor antagonists.[13]

In a recent paper,[14] we reported the synthesis and the pharmacological characterization of the racemic form of the two acidic bicyclic amino acids, 5-amino-4,5,6,6a-tetrahydro-3a*H*-cyclopenta[*d*]isoxazole-3,5-di-

† Dedicated to the memory of Professor Giorgio Bianchi.

* To whom correspondence should be addressed. Phone: +39 02 50317538. Fax: +39 02 50317574. E-mail: carlo.demicheli@unimi.it.

‡ Istituto di Chimica Farmaceutica.

§ Department of Medicinal Chemistry.

Department of Molecular Biology.

⊥ Dipartimento di Farmacologia Preclinica e Clinica.

⊗ Laboratoire de Chimie et Biochimie Pharmacologiques et Toxicologiques.

10.1021/jm0504499 CCC: $30.25
Published on Web 09/13/2005

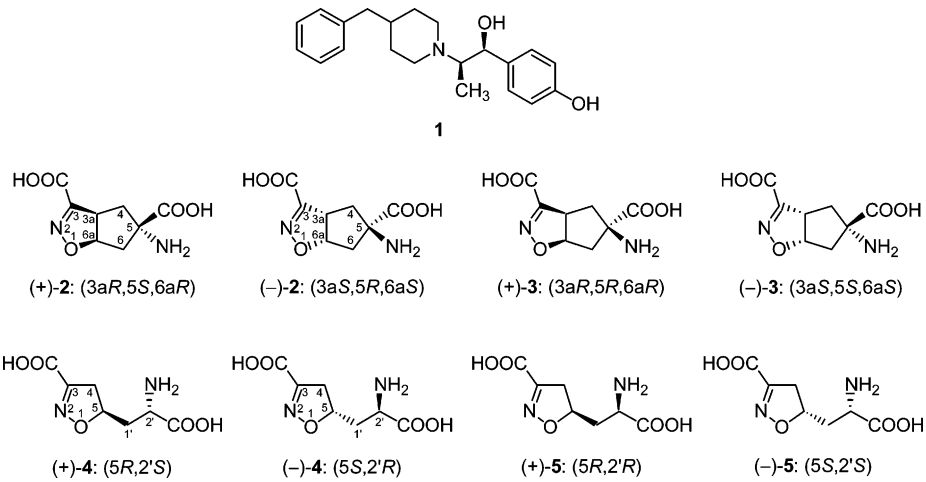

Figure 1. Structures of ifenprodil (**1**) and target compounds.

carboxylic acids (±)-**2** and (±)-**3** (Figure 1). Derivative (±)-**2** behaved as a quite potent NMDA receptor antagonist supported by antagonist activity at mGluR1,5 (group I) and agonist activity at mGluR2. This pharmacological profile candidates (±)-**2** as a new lead for neuroprotective agents. The four stereoisomers (+)-**2**, (−)-**2**, (+)-**3**, and (−)-**3** were subsequently prepared and the absolute configuration assigned by vibrational circular dichroism analyses.[15] The structure−activity relationship of (±)-**2** was extended through the synthesis of monocyclic analogues, 5-(2-amino-2-carboxyethyl)-4, 5-dihydroisoxazole-3-carboxylic acids (±)-**4** and (±)-**5**, and evaluation of their biological activity. Both racemates were endowed with a remarkable NMDA antagonist activity devoid of any activity at mGluRs.[16]

This paper reports the synthesis of the four stereoisomers (+)-**4**, (−)-**4**, (+)-**5**, and (−)-**5** and the results of pharmacological investigations of the eight enantiomers (+)-**2**, (−)-**2**, (+)-**3**, (−)-**3**, (+)-**4**, (−)-**4**, (+)-**5**, and (−)-**5**. The pharmacology at iGluRs and mGluRs was studied by in vitro binding to rat cortical membranes and by measurement of functional activity in second messenger assays at cloned receptors expressed in Chinese hamster ovary cells, respectively. The neuroprotective effects of the most promising derivatives were then evaluated in an in vitro model of cerebral ischemia on murine cortical cells exposed to oxygen and glucose deprivation (OGD). Furthermore, compounds (+)-**2**, (−)-**4**, and (+)-**5**, being NMDA receptor antagonists, were assayed using *Xenopus* oocytes expressing cloned rat NMDA receptors containing NR1 in combination with either NR2A, NR2B, NR2C, or NR2D, to investigate subunit selectivity. The overall results of the pharmacological investigations have been accounted for by docking the compounds in the binding site of an NR2A antagonist model[17] as well as in an mGluR2 agonist model.[18]

Chemistry

The key step in the synthesis of target compounds (+)-**4**/(−)-**4** and (+)-**5**/(−)-**5** is the enzymatic resolution of the previously reported isoxazoline derivatives (±)-**6** and (±)-**7**.[16] As shown in Tables 1 and 2, derivatives (±)-**6** and (±)-**7** were hydrolyzed in the presence of a number of commercially available enzymes. Among the tested biocatalysts, Proleather turned out to be the most selective enzyme for substrate (±)-**6** (Table 1), able to efficiently hydrolyze the 2′ methyl ester of enantiomer (+)-**6** to the corresponding monoacid (+)-**8** (Scheme 1). It is worth pointing out that the reaction spontaneously subsided at 50% conversion and was characterized by a high degree of enantio-discrimination (E > 1000).[19] As shown in Table 2, the same set of reactions performed on derivative (±)-**7** demonstrated that Papain, Proleather, and Acylase were equally efficient to hydrolyze enantiomer (−)-**7** to monoacid (−)-**9** (Scheme 1). Since Papain, among these three enzymes, is less expensive, we used this enzyme in the preparation of (−)-**5** and (+)-**5**.

Intermediates (−)-**6**, (+)-**8**, (+)-**7**, and (−)-**9** were converted into target amino acids (−)-**4**, (+)-**4**, (+)-**5**, and (−)-**5**, respectively, through standard transformations (Scheme 1). Chiral HPLC analyses carried out on final amino acids showed that all the compounds were provided with a value of enantiomeric excess higher

Table 1. Enzymatic Hydrolyses Carried out on Diester (±)-**6**

enzyme	ee[a] of (+)-(5*R*,2′*S*)-**8**	degree of conversion (%)	*E* value[b]
α- chymotrypsin	99	30	300
CAL-A	n.r.[c]	=	=
papain	99	30	300
lipase PS	n.r.	=	=
proleather	≥ 99	50	>1000
CAL-B	n.r.	=	=
acylase	95.6	50	105
PPL	n.r.	=	=
lipase AK	n.r.	=	=

[a] Enantiomeric excess. [b] E: enantiomeric ratio, calculated according to the equations reported in ref 19. [c] n.r.: no reaction.

Table 2. Enzymatic Hydrolyses Carried out on Diester (±)-**7**

enzyme	ee[a] of (−)-(5*S*,2′*S*)-**9**	degree of conversion (%)	*E* value[b]
α-chymotrypsin	n.r.[c]	=	=
CAL-A	n.r.	=	=
papain	≥ 99	50	>1000
lipase PS	n.r.	=	=
proleather	≥ 99	50	>1000
CAL-B	n.r.	=	=
acylase	≥ 99	50	>1000
PPL	n.r.	=	=
lipase AK	n.r.	=	=

[a] Enantiomeric excess. [b] E: enantiomeric ratio, calculated according to the equations reported in ref 19. [c] n.r.: no reaction.

Scheme 1[a]

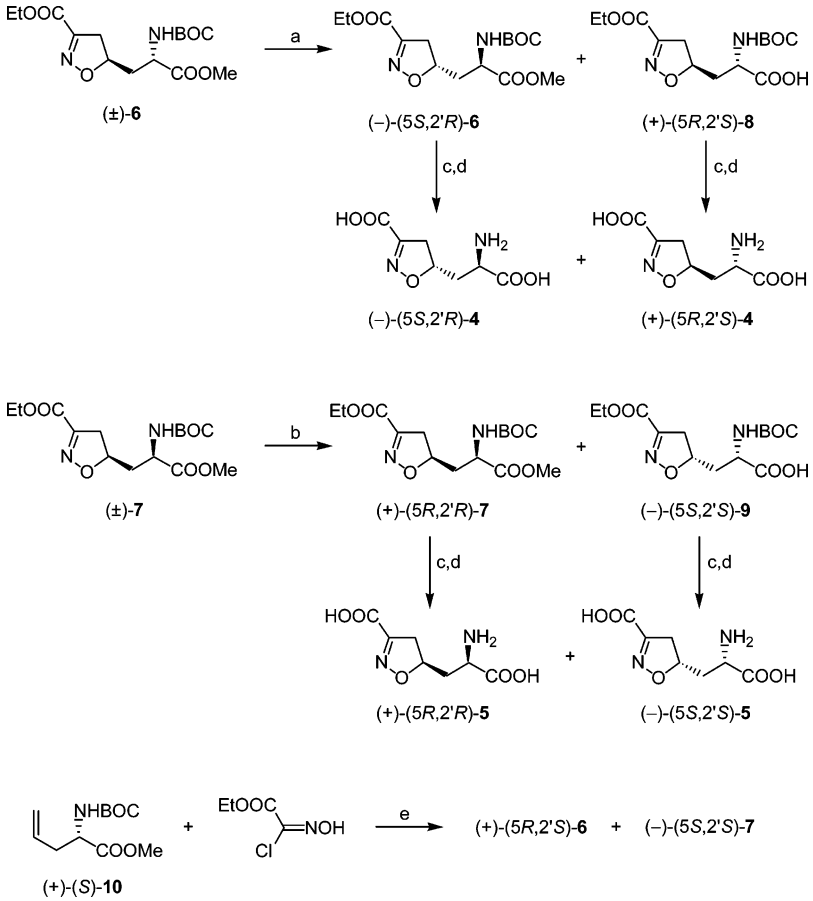

[a] (a) Proleather, 0.1 M phosphate buffer/acetone; (b) Papain, 0.1 M phosphate buffer/acetone; (c) 1 N NaOH/H_2O−EtOH; (d) 30% CF_3CO_2H/CH_2Cl_2; (e) $NaHCO_3$/AcOEt.

Table 3. Rat Cortical Membrane Receptor Binding and in Vitro Electrophysiological Data from the Rat Cortical Wedge Preparation[a]

	receptor binding			
compd	[^{3}H]CGP 39653 K_i (μM)	[^{3}H]AMPA IC_{50} (μM)	[^{3}H]KA IC_{50} (μM)	electrophysiology (rat cortical wedge): antagonism,[b] IC_{50} (μM)
(±)-**2**[c]	0.37 [0.34; 0.40]	>100	>100	14 ± 2
(+)-**2**	0.233 [0.230; 0.237]	>100	>100	
(−)-**2**	47 [43; 51]	>100	>100	
(±)-**3**[c]	>100	>100	>100	
(±)-**4**[d]	0.21 [0.18; 0.23]	>100	>100	14.2 [12.9;15.7]
(+)-**4**	1.9 [1.8; 2.0]	>100	>100	
(−)-**4**	0.10 [0.09; 0.12]	>100	>100	
(±)-**5**[d]	0.96 [0.88; 1.1]	>100	>100	30.5 [24.9;37.4]
(+)−**5**	0.51 [0.49; 0.53]	>100	>100	
(−)-**5**	2.5 [2.4;2.7]	>100	>100	

[a] Values are expressed as the antilog to the log mean of three individual experiments. Numbers in parentheses [min; max] indicate ± SEM according to a logarithmic distribution. [b] Antagonism of NMDA (10 μM) induced responses. [c] Data from ref 14. [d] Data from ref 16.

than 99%. Since the relative stereochemistry of amino acids (±)-**4** and (±)-**5** was previously assigned by X-ray analysis,[16] the absolute configuration of the stereogenic centers of the pairs of amino acids (−)-**4**/(+)-**4** and (+)-**5**/(−)-**5** was assigned by chemical correlation with enantiopure dipolarophile (+)-**10**. To this end, 1,3-dipolar cycloaddition of (*S*)-(+)-*N*-BOC allylglycine methyl ester [(+)-**10**][20] to ethoxycarbonylformonitrile oxide, generated in situ by treatment of ethyl 2-chloro-2-(hydroxyimino)acetate[21] with a base (Scheme 1), yielded a 2:3 mixture of the stereomeric cycloadducts (+)-(5*R*,2′*S*)-**6** and (−)-(5*S*,2′*S*)-**7**.

Results and Discussion

The three pairs of acidic amino acids (+)-**2**/(−)-**2**, (+)-**4**/(−)-**4** and (+)-**5**/(−)-**5** were assayed in vitro by means of receptor binding to rat cortical membranes using the radioligands [^{3}H]CGP 39653, [^{3}H]AMPA and [^{3}H]KA as representatives for NMDA, AMPA and KA receptors, respectively[22−24] (Table 3). The enantiomers (+)-**3** and (−)-**3** were not tested in these binding assays due to the lack of affinity of the racemate (±)-**3**. The pairs of enantiomers (+)-**2**/(−)-**2** and (+)-**3**/(−)-**3**, whose racemates displayed activity at mGluRs,[14] were assayed at rat mGluR1 (representative of group I), at mGluR2

Table 4. Activities at Cloned Rat mGlu Receptors Expressed in CHO Cells[a]

	mGluR1		mGluR2		mGluR4	
compd	EC_{50} (μM)	K_i (μM)	EC_{50} (μM)	K_i (μM)	EC_{50} (μM)	K_i (μM)
(±)-**2**[b]		94 ± 16	*c*		>1000	>1000
(+)-**2**	>1000	>1000	>1000	>1000	>1000	>1000
(−)-**2**		95 ± 13	weak		>1000	>1000
(±)-**3**[b]		27 ± 7	16 ± 3[d]		>1000	>1000
(+)-**3**		33 ± 6	9.1 ± 0.8[e]		weak	
(−)-**3**	>1000	>1000	>1000	>1000	>1000	>1000
(±)-**4**[f]	>1000	>1000	>1000	>1000	>1000	>1000
(±)-**5**[f]	>1000	>1000	>1000	>1000	>1000	>1000

[a] Data are given as mean ± SEM of at least three independent experiments. [b] Data from ref 14. [c] 1 mM concentration produces a 36 ± 7% activation. [d] Max. = 59±7%. [e] Max. = 42±4%. [f] Data from ref 16.

(representative of group II) and at mGluR4 (representative of group III); all the receptors were expressed in CHO cells (Table 4).[25] Due to inactivity of the racemates,[16] the enantiomers (+)-**4**, (−)-**4,** (+)-**5**, and (−)-**5** were not tested on mGluRs.

As shown in Table 3, the NMDA receptor activity, previously observed for racemates (±)-**2**, (±)-**4**, and (±)-**5**,[14,16] can be attributed to the enantiomers (+)-**2**, (−)-**4**, and (+)-**5**, respectively. Similarly, the mGluR activity of derivatives (±)-**2**, and (±)-**3** (Table 4),[14] resides exclusively in the enantiomers (−)-**2** and (+)-**3**, respectively. As a consequence, the mixed activity at mGluRs and NMDA receptors of racemate (±)-**2** is the overlap of the NMDA antagonist activity of its enantiomer (+)-**2** with the mGluR activity of enantiomer (−)-**2**.

To evaluate the subtype selectivity of derivatives (+)-**2**, (−)-**4**, and (+)-**5** on cloned rat NMDA receptors, they were tested on *Xenopus* oocytes expressing NR1 in combination with either NR2A, NR2B, NR2C, or NR2D subunits. The antagonists were tested at concentrations of 0.3 μM and 3 μM for inhibition of currents evoked by 10 μM Glu (Figure 2). At concentrations of 3 μM, all three derivatives antagonized responses from NR2A and NR2B subtypes, and they showed no antagonistic effects on NR2C and NR2D subtypes. This shows that the three antagonists have a preference for NR2A and NR2B subtypes, as the potency of Glu at the four receptor subtypes is similar (Glu EC_{50}-values of NR1/NR2A,[26] NR1/NR2B,[26] NR1/NR2C,[26] and NR1/NR2D are 2.9 μM, 1.8 μM, 1.5 μM, and 0.5 μM, respectively, data not shown). Derivative (−)-**4** seems to be more potent than (+)-**2** and (+)-**5** since only this compound antagonizes NR2A at concentrations of 0.3 μM. The results of this investigation show that (+)-**2**, (−)-**4**, and (+)-**5** share similar NMDA receptor subtype selectivity preferring NR2A and NR2B over NR2C and NR2D (and that the order of potency [(−)-**4** > (+)-**2** = (+)-**5**)] is similar though not identical to the order of affinity obtained from binding to rat cortical membranes (Table 3).

The neuroprotective effects of selected derivatives were evaluated in cultured murine cortical cells exposed to OGD, an in vitro model of cerebral ischemia (Figures 3 and 4). Exposure to OGD for 60 min produced an intermediate level of neuronal damage, measured by the release of lactate dehydrogenase (LDH) into the bathing

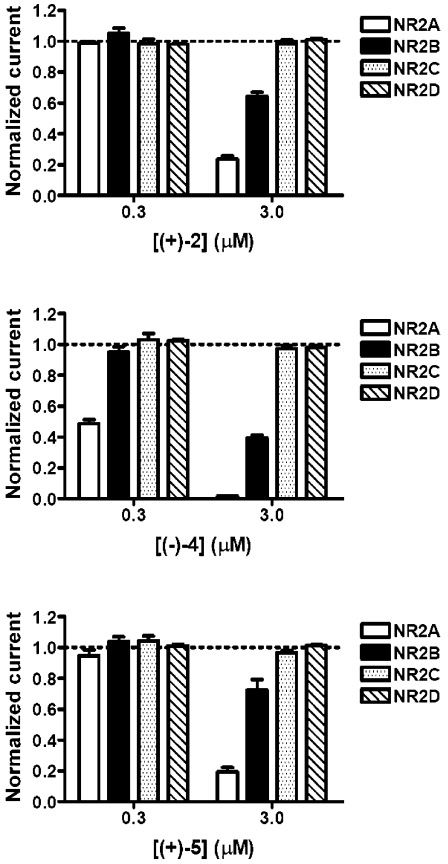

Figure 2. Derivatives (+)-**2**, (−)-**4**, and (+)-**5** were tested at concentrations of 0.3 μM and 3 μM for inhibition of currents evoked by 10 μM Glu on *Xenopus* oocytes expressing cloned rat NMDA receptors containing NR1 in combination with either NR2A, NR2B, NR2C, or NR2D. The responses are normalized to the response from 10 μM Glu.

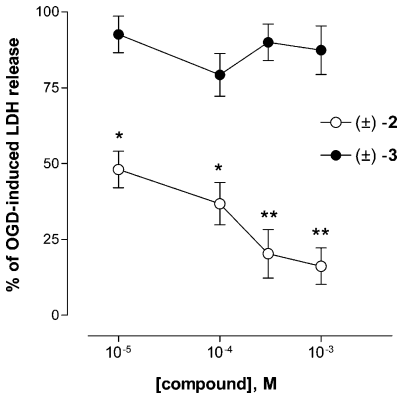

Figure 3. Neuroprotection by derivatives (±)-**2** and (±)-**3** against OGD-induced neurotoxicity in murine cortical cultures. Data are expressed as percent of OGD-induced neuronal damage. Each point represents the mean ± SEM of three experiments. *, $p < 0.05$ and **, $p < 0.01$ versus OGD (ANOVA + Tukey's w test).

medium, which was approximately 75% of that observed by exposing the cultures to 1 mM Glu (data not shown).[27]

None of the tested compounds produced any significant change in the release of LDH when added alone into the incubation medium (not shown). When added to the incubation medium during OGD and the subsequent 24 h recovery period, compound (±)-**2**, but not compound (±)-**3**, dose-dependently attenuated OGD-

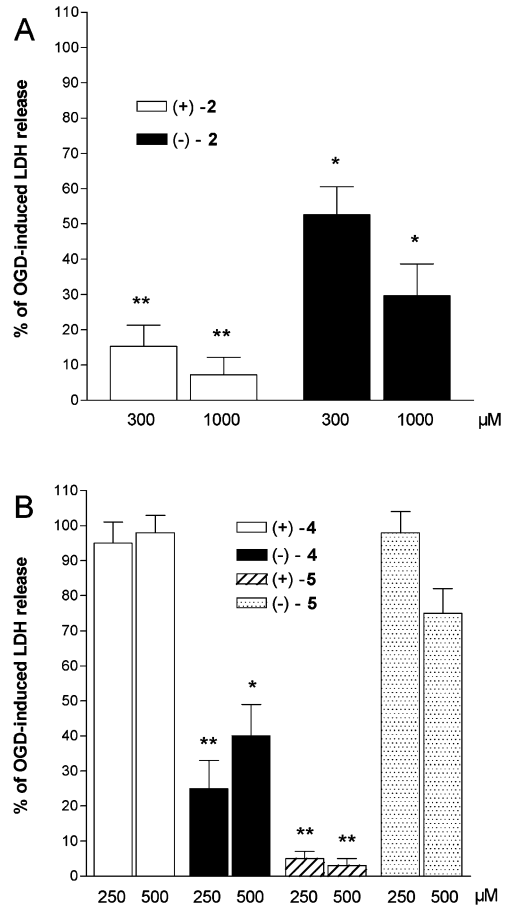

Figure 4. Neuroprotective effects of (A) enantiomers (+)-**2** and (−)-**2** and (B) enantiomers (+)-**4**, (−)-**4**, (+)-**5**, and (−)-**5** against OGD-induced neurotoxicity in murine cortical cultures. Data are expressed as percent of OGD-induced neuronal damage. Each bar represents the mean ± SEM of three experiments. *, $p < 0.05$ and **, $p < 0.01$ versus OGD (ANOVA + Tukey's w test).

induced neuronal death (Figure 3). The maximal effect was observed at 300−1000 μM. When (+)-**2** and (−)-**2** were tested, enantiomer (+)-**2** displayed a greater neuroprotective effect than (−)-**2** (Figure 4A), which is compatible with the fact that (+)-**2** has high affinity for NMDA receptors whereas (−)-**2** has weak affinity for NMDA receptors and weak antagonist activity at mGluR1 receptors. Similarly, among (±)-**4** and (±)-**5** enantiomers, the compounds displaying the most potent activity as NMDA receptor antagonists, (−)-**4** and (+)-**5**, were those that provided the most pronounced neuroprotective effect (Figure 4B).

An overview of the results reported in Tables 3 and 4 displays the remarkable enantiopharmacology of the compounds under study. Indeed, the activity displayed by (±)-**2** at both NMDA and mGluRs is a combination of a high affinity of enantiomer (+)-**2** for NMDA receptors with a weak activity of its antipode (−)-**2** at both mGluRs and NMDA receptors. In the remaining cases, the biological activity of the racemates resides solely in one enantiomer, i.e., the mGluRs activity of (±)-**3**, is due to the (+)-**3** enantiomer, whereas enantiomers (−)-**4** and (+)-**5** carry the NMDA antagonist activity of the corresponding racemates (±)-**4** and (±)-**5**. These data are further confirmed in the neuroprotective test (Figures 3 and 4), where the eutomers turned out to be (+)-**2**, (−)-**4**, and (+)-**5**. Worth noting is that the neuroprotective effect can be evidenced solely for derivatives provided with high affinity for the NMDA receptor binding site. Since a neuroprotective effect mediated by mGluRs has been reported, the inefficacy of derivatives (−)-**2** and (+)-**3** may be attributed to their low activity at mGluR1,5 coupled to a marginal activity at mGluR2.

To get insights into the relationship between stereochemistry and biological activity, we performed docking studies on the NMDA antagonists (+)-**2**, (−)-**4**, and (+)-**5** into the recently proposed homology model of the NR2A.[17] Computational studies essentially confirm the results reported for the 2-amino-5-phosphonopentanoic acid (AP5-)-like NMDA-selective antagonists. Since the amino acidic moieties of (+)-**2**, (−)-**4**, and (+)-**5** adopt the same binding mode, they were docked in accordance to the mutational analysis reported for the NR2A subunit.[28,29] The flexible docking calculations reveal that the carboxylic group interacts through a salt bridge with the side chain of R518 and, in addition, a hydrogen bond involving T513 stabilizes the ligand docking into the pocket (Figure 5). At the same time, the amino group gives rise to supplementary links with the backbone of S511 residue and the side chains of amino acids T513, H485, and D731. In our previous study,[17] we assumed that a crucial salt bridge interaction into the binding site should involve the ligand distal carboxylic group and residues S689−T690. This region of the receptor protein constitutes the amino terminal portion of an α-helix, and, as has been shown,[30] it generates a positively charged macro dipole which attracts negatively charged moieties of the ligands (Figure 5). As a consequence, the distal acidic group of the isoxazoline ring of amino acids (+)-**2**, (−)-**4**, and (+)-**5** is suitably oriented to interact with the backbone NH groups of the protein residues S689−T690. On the other hand, the rigidity of enantiomer (−)-**2** prevents a productive interaction between the ω-CO_2H group and the amino terminal portion of the above-described α-helix.

The rank order in the flexible docking of the antagonists under investigation is in good agreement with the rank order of their experimental binding affinities. Moreover, going from (*R*)-AP5 to 2-amino-4-oxo-5-phosphono-pentanoic acid [MDL 100,453] (Figure 6), both NMDA selective antagonists, a doubling of the binding affinity was reported,[2] which parallels the results observed for derivatives (+)-**2** and (−)-**4**. This outcome may be rationalized by admitting an extra hydrogen bond between the MDL 100,453 carbonyl group and the side chain of the Y730 residue. Indeed, docking studies on compound (−)-**4** indicate the same additional hydrogen bond. In this case, the electron donor oxygen atom of the isoxazoline ring of (−)-**4** is capable to interact with the OH group of Y730, mimicking the carbonyl group of MDL 100,453. Due to the opposite absolute configuration at position 5, stereoisomer (+)-**5** has a weaker interaction with Y730, expressed by the lower affinity, compared to (−)-**4**, which parallels the low score obtained in the docking calculations.

Furthermore, the enantiomers (+)-**2**, (−)-**2**, (+)-**3**, and (−)-**3**, which are agonists or partial agonists at mGluR2 (Table 4), were analyzed using molecular modeling tools.[18] Among the four pairs of tested enantiomers, only

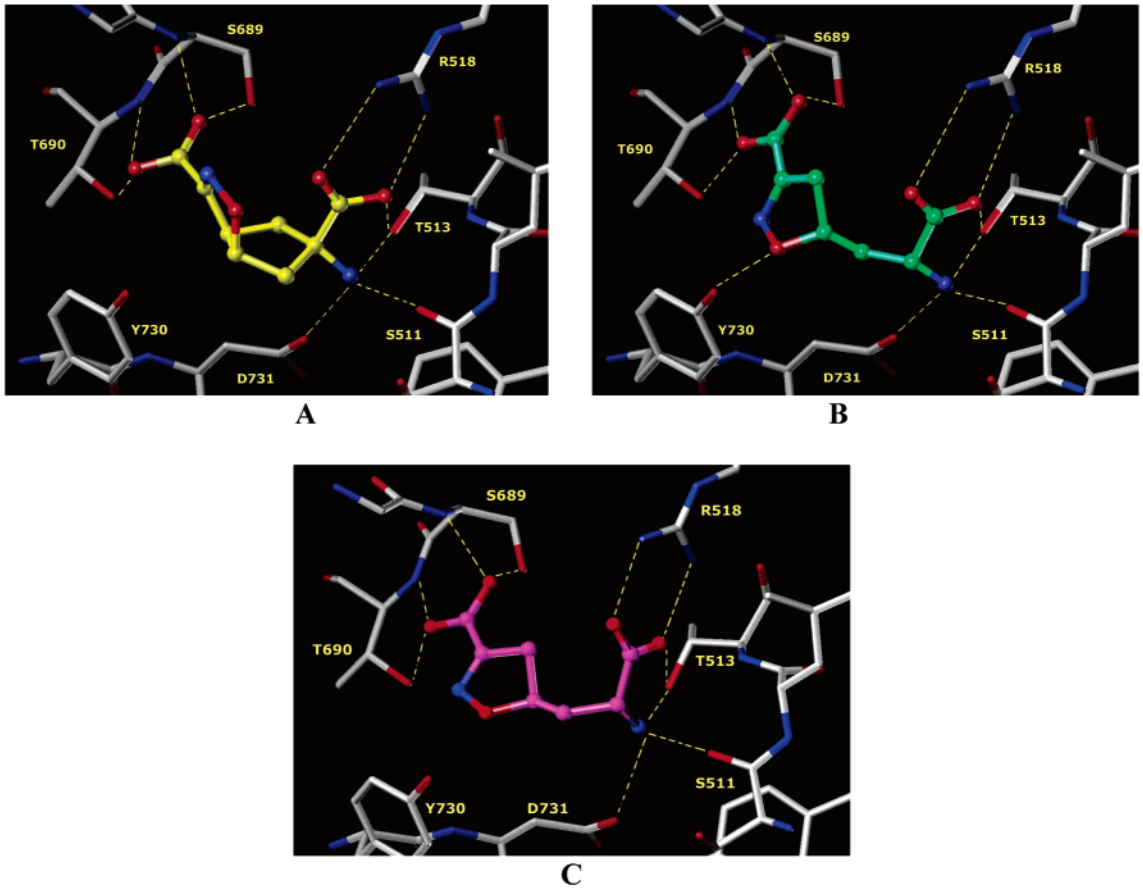

Figure 5. Docking of the new NMDA selective antagonists into the model of the NR2A subunit. (A) (+)-**2**; (B) (−)-**4**; (C) (+)-**5**. The ligands are displayed as ball-and-stick models whereas amino acids involved in the ligand binding are in capped sticks color code.

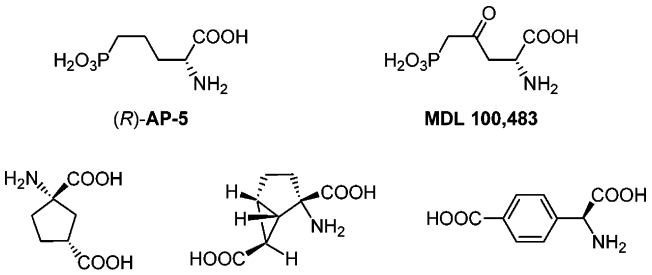

Figure 6. Structure of selective NMDA receptor antagonists (top) and selective mGlu2R agonists (bottom).

two displayed agonist activity at one subtype of mGluRs (mGluR2). Conformational analysis by high-temperature molecular dynamics[31] showed that (−)-**2** and (+)-**3** adopt one stable conformation while (+)-**4**/(−)-**4** and (−)-**5**/(+)-**5** are more flexible and assume conformations different from that of (−)-**2** and (+)-**3**. Worth mentioning, enantiomers (−)-**2** and (+)-**3** adopt an extended conformation that fits the agonist pharmacophore model that was previously generated.[31] Superimposition of the enantiomers to the mGluR2 agonist pharmacophore model reveals that (−)-**2** and (+)-**3** are expected to be the active enantiomers, since their cyclopentane rings are located in the same region as those of known agonists as (1*S*,3*R*)-1-amino-1,3-cyclopentanedicarboxylic acid [(1*S*,3*R*)-ACPD] and 2-aminobicyclo[3.1.0]hexane-2,6-dicarboxylic acid [LY354740] (Figures 6 and 7). The enantiomers (+)-**2** and (−)-**3** occupy a region where substituents are poorly tolerated as defined in the mGluR2 pharmacophore model[31] and illustrated with (−)-**3** and (1*R*,3*S*)-ACPD in Figure 7. Distances between amino and carboxylic functions at position 5 (proximal functions) and carboxylate at position 3 (distal function) are larger for **2** and **3** than those tolerated at the mGluR1 binding site; this may explain their antagonist properties. Indeed, a similar mGluR selectivity was noted for phenylglycines such as (*S*)-4-carboxyphenylglycine [(*S*)-4CPG] (Figure 6), which exhibits similar functional group distances, agonist activity at mGluR2, and antagonist activity at mGluR1.[18] However, although functional groups of **2** and **3** are well positioned for mGluR2 activation, variable potencies have been detected. These differences may result from steric restrictions at the binding site. In Figure 7A, the heterocycle of (−)-**2** lines a forbidden region situated between the two acidic features of the model[31] and may be responsible for the weak agonist activity.

Observations on pharmacophore models can be correlated with those on homology models docked with the agonists. The (−)-**2** and (+)-**3** isomers were docked in the mGluR2 homology model that was previously generated.[18] Functional groups of agonists were superimposed to those of Glu in the 3D-homology model, and the resulting system was minimized. The amino terminal domain (ATD) of mGluRs folds in two lobes linked by a hinge (Figure 8A). The agonists bind to lobe-I and are then trapped upon closing of the second lobe.[32] The

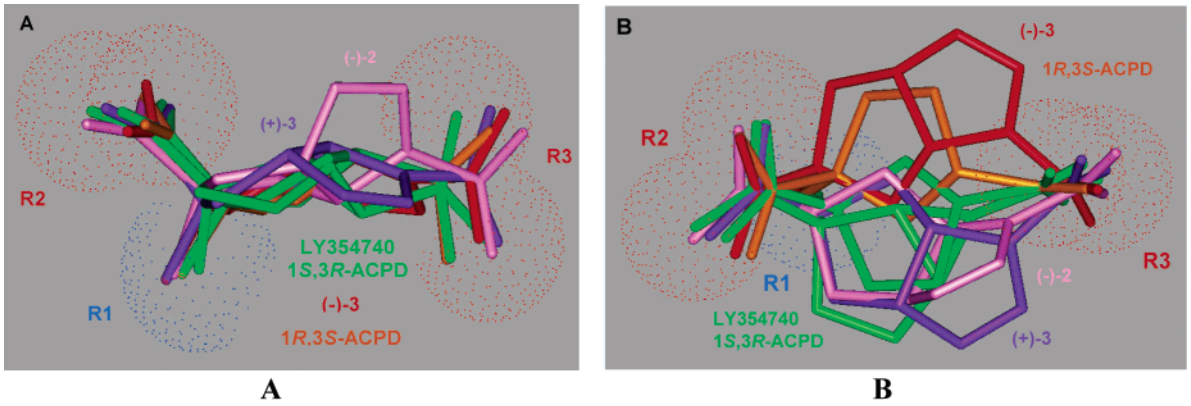

Figure 7. (A) Side view of mGlu2R pharmacophore model from ref.[31] with (−)-**2** (pink) and (+)-**3** (purple) superimposed. Potent agonists [LY354740 and (1*S*,3*R*)-ACPD] are colored in green, moderate activity agonist [(1*R*,3*S*)-ACPD)] in orange, and inactive analogue [(−)-**3**] in red. van der Waals spheres of oxygen and nitrogen atoms of proximal and distal functions are displayed as red and blue dotted spheres, respectively, marking the ionizable features of the pharmacophore model (R2, R3, and R1). (B) Top view of part A.

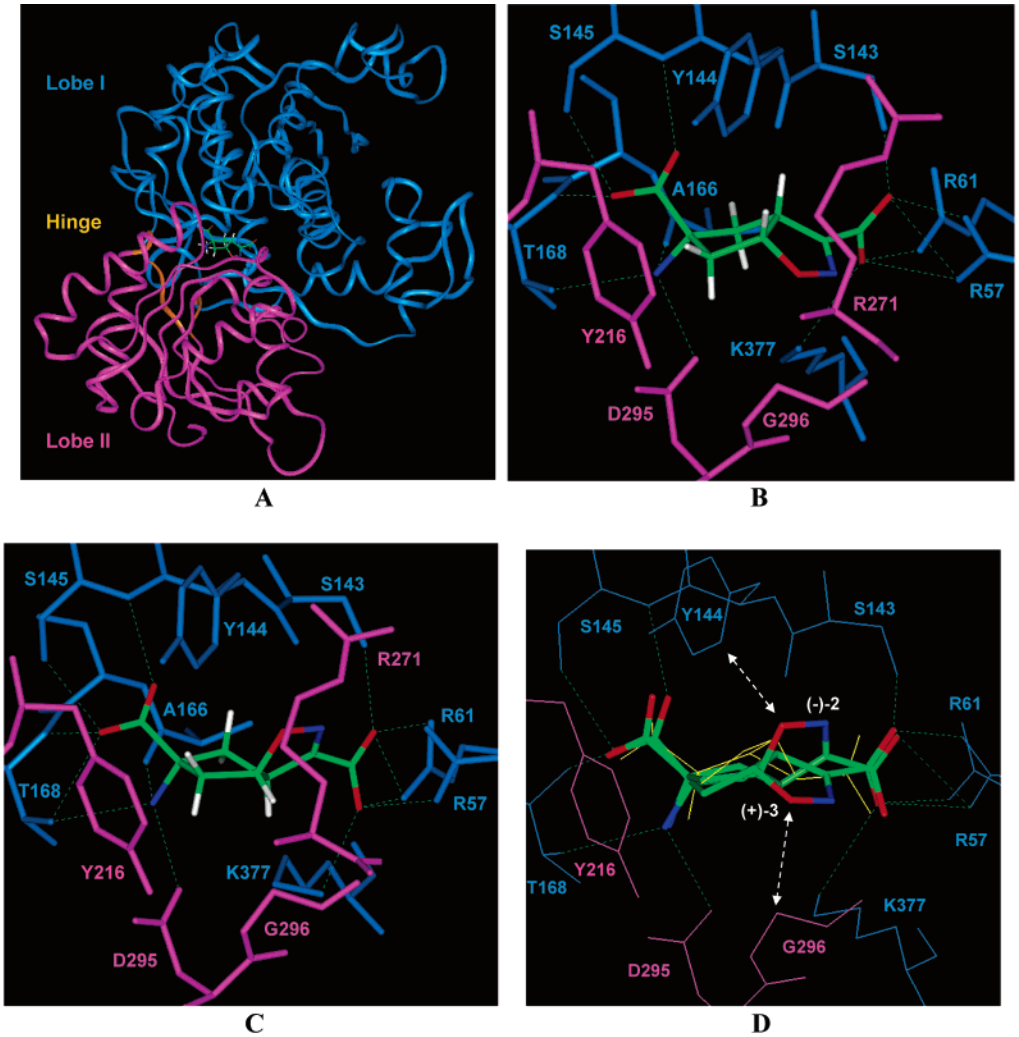

Figure 8. (A) 3D-Homology model of the ATD of mGlu2R docked with (+)-**3**.[18] Lobe-I is colored in blue, lobe-II in magenta, and the hinge in orange. Color code for the ligand: carbons in green, oxygens in red, nitrogens in blue. (B) Expanded view of part A, with the same color code. (C) Expanded view of the docking of (−)-**2** in the mGlu2R homology 3D-model; color code as in part A. (D) Superimposition of (−)-**2**, (+)-**3**, and LY354740 (yellow) docked in the mGlu2R binding site. Steric interactions are indicated with white arrows; color code as in part A.

closed conformation of the ATD induces receptor activation. In Figure 8A, the mGluR2 ATD docked with the most potent agonist (+)-**3** is displayed. An expanded view of the binding site bound with (+)-**3** and (−)-**2** is shown in Figure 8, parts B and C. For comparison, docking of LY354740 is displayed in Figure 8D. In the two models, the proximal functions of (+)-**3** and (−)-**2** are bound to the conserved residues T168, S145, CO of

A166 (lobe-I), and Y216, D295 (lobe-II) as described for all mGluR agonists.[18,33] The distal functions bind to the same cluster of basic (R57, R61, K377) and hydrophilic (S143) residues from lobe-I, as for other potent mGluR2 agonists. No distal bindings to lobe-II are detected; however, water molecules can bridge the ligand to the backbone or side chains of lobe II.[18] The side chain of R271 is also making van der Waals contacts with the bicyclic structures of (−)-**2** and (+)-**3** as for LY354740. Compound (+)-**3** is a partial agonist, and this property may be due to the steric bulk of the heterocycle, which can come into steric interaction with G296 of lobe-II, upon closing of the bilobate ATD (Figure 8D). We have previously shown that such an interaction may be the reason for antagonist properties of some ligands.[34] In the case of (+)-**3**, optimal closing is not reached; however, the steric hindrance is not as drastic as with α-alkylated ligands. In regards to (−)-**2**, its weak agonist activity may be also related to the steric bulk of its heterocycle. Yet because of a different configuration at the bicyclic junction, this cycle is facing lobe-I. Steric hindrance with side chains and backbone of lobe-I residues may result in poor binding to lobe-I (Figure 8D) and consequently weaker potency.

In conclusion, we have investigated the pharmacology of four pairs of acidic amino acids (+)-**2**/(−)-**2**, (+)-**3**/(−)-**3**, (+)-**4**/(−)-**4**, and (+)-**5**/(−)-**5** and showed that the pharmacological activity is strictly related to their absolute stereochemistry. In fact, in the case of compounds (±)-**3**, (±)-**4**, and (±)-**5**, only one enantiomer possess biological activity, and, even more interestingly, in the case of (±)-**2**, the two enantiomers display selectivity for the NMDA receptors and for the mGlu receptors, respectively.

The results were rationalized by means of molecular modeling studies. By using a homology model of the NR2A subunit of the NMDA receptors, we have found that the rank order in the flexible docking of the antagonists (+)-**2**, (−)-**4**, and (+)-**5** is comparable to the rank order of their experimental binding affinities. The higher affinity displayed by (−)-**4**, compared to the other two derivatives, can be explained by an extra hydrogen bond between the electron donor oxygen atom of the isoxazoline ring and the OH group of Y730.

On the other hand, the analysis of the mGluR2 agonist pharmacophore model shows that (−)-**2** and (+)-**3**, which are weak or partial agonists, respectively, locate their cyclopentane rings in the same region as those of known agonists as (1S,3R)-ACPD and LY354740, while the inactivity of their enantiomers (+)-**2** and (−)-**3** can be explained by the fact that they occupy a region where substituents are poorly tolerated. Moreover, the weak agonist activity of (−)-**2**, as well as the partial agonism of (+)-**3**, seem to be due to the steric bulk of their heterocyclic moieties. These results correlate well with those obtained by docking the compounds in the homology model of the mGluR2.

Experimental Section

Material and Methods. (*S*)-(−)-2-Amino-4-pentenoic acid was purchased from Fluka. Lipase B from *Candida antarctica* (CALB) was bought from Roche Diagnostics (CHIRAZYME L-2). Chymotrypsin, papain from *Carica papaya*, porcine pancreatic lipase (PPL), lipase from *Pseudomonas cepacia* (lipase PS), lipase A from *Candida antarctica* (CALA), and acylase were purchased from Fluka. Proleather (Subtilysin Carlsberg) and lipase AK were obtained from Amano Pharmaceuticals Co.

^{1}H NMR and ^{13}C NMR spectra were recorded with a Varian Mercury 300 (300 MHz) spectrometer in $CDCl_3$ or D_2O solution at 20 °C. Chemical shifts (δ) are expressed in ppm and coupling constants (J) in hertz. HPLC analyses were performed with a Jasco PU-980 pump equipped with a UV−vis detector Jasco UV-975 and with a Sedex 750 light scattering detector. Rotary power determinations were carried out with a Perkin-Elmer 241 polarimeter coupled with a Haake N3-B thermostat. TLC analyses were performed on commercial silica gel 60 F_{254} aluminum sheets; spots were further evidenced by spraying with a dilute alkaline potassium permanganate solution or with ninhydrin. Melting points were determined on a model B 540 Büchi apparatus and are uncorrected. Microanalyses (C, H, N) of new compounds agreed with the theoretical value within ±0.3%.

Ethyl (5*R,2′*S**)-5-(2-*tert*-Butoxycarbonylamino-2-methoxycarbonylethyl)-4,5-dihydroisoxazole-3-carboxylate [(±)-6] and Ethyl (5*R**,2′*R**)-5-(2-*tert*-Butoxycarbonylamino-2-methoxycarbonylethyl)-4,5-dihydroisoxazole-3-carboxylate [(±)-7].** Cycloadducts (±)-**6** and (±)-**7** were prepared according to the procedure previously reported.[16] HPLC retention times of the pairs of enantiomers are the following. (−)-**6**: 17.36 min; (+)-**6** 19.88 min (column: CHIRALCEL OD-H, Diacel; eluent: petroleum ether/2-propanol 97:3; flow rate: 1.0 mL/min; λ = 254 nm). (−)-**7**: 30.23 min; (+)-**7** 33.67 min (column: CHIRALCEL OD-H, Diacel; eluent: petroleum ether/2-propanol 95:5; flow rate: 1.0 mL/min; λ = 254 nm).

General Procedure for the Analytical Enzymatic Hydrolyses of Diesters (±)-6 and (±)-7. To a suspension of (±)-**6** [or (±)-**7**] (5 mg, 0.015 mmol) in 0.1 M phosphate buffer pH 7.0 (1 mL) and acetone (200 μL) was added the enzyme (5 mg), and the mixture was stirred at room temperature. The outcome of the reaction was monitored by HPLC; every hour, 20 μL of the mixture were withdrawn, made acidic with 2 N HCl (10 μL), and extracted with ethyl acetate (20 μL). The organic phase was analyzed by chiral HPLC under the protocol described above.

Preparative Enzymatic Hydrolysis of Substrate (±)-6. To a suspension of (±)-**6** (750 mg, 2.18 mmol) in 0.1 M phosphate buffer pH 7.0 (8 mL) and acetone (2 mL) was added Proleather (1.0 g), and the mixture was gently stirred at room temperature for 2 h. The progress of the reaction was monitored by chiral HPLC (column: CHIRALCEL OD-H, Diacel; eluent: petroleum ether/2-propanol 97:3; flow rate: 1.0 mL/min; λ = 254 nm). The reaction spontaneously stopped at 50% conversion to yield monoacid (+)-**8** and residual ester (−)-**6** in e.e. higher than 99%. Solid $NaHCO_3$ was added, and then the reaction mixture was extracted with diethyl ether and the pooled organic layers were evaporated to recover the residual ester (−)-**6** (345 mg). The aqueous phase was made acidic with 2 N HCl, and the monoacid (+)-**8** (315 mg) was obtained after extraction with diethyl ether, drying over anhydrous Na_2SO_4, and evaporation of the solvent.

Ethyl (5*S*,2′*R*)-5-(2-*tert*-Butoxycarbonylamino-2-methoxycarbonylethyl)-4,5-dihydroisoxazole-3-carboxylate (−)-6: $[\alpha]^{20}_D$: −71.2 (*c* 1.0, chloroform); colorless oil; Anal. ($C_{15}H_{24}N_2O_7$) C, H, N. Spectroscopic data agreed with those reported for the corresponding racemate.[16]

Ethyl (5*R*,2′*S*)-5-(2-*tert*-Butoxycarbonylamino-2-carboxyethyl)-4,5-dihydroisoxazole-3-carboxylate (+)-8: $[\alpha]^{20}_D$: +54.8 (*c* 1.0, methanol); colorless oil; R_f 0.62 (chloroform/methanol 9:1 + 50 μl acetic acid). HPLC retention time: 24.77 min (column: CHIRALCEL OD-H, Diacel; eluent: petroleum ether/2-propanol 97:3; flow rate: 1.0 mL/min; λ = 254 nm). ^{1}H NMR ($CDCl_3$): 1.36 (t, J = 7.3, 3H), 1.43 (s, 9H), 2.20 (m, 2H), 2.94 (dd, J = 7.3, 17.5, 1H), 3.38 (dd, J = 11.3, 17.5, 1H), 4.32 (q, J = 7.3, 3H), 4.34 (m, 1H), 4.98 (m, 1H), 5.38 (bd, J = 6.2, 1H); Anal. ($C_{14}H_{22}N_2O_7$) C, H, N.

Preparative Enzymatic Hydrolysis of Substrate (±)-7. To a suspension of (±)-**7** (1.0 g, 2.90 mmol) in 0.1 M

phosphate buffer pH 7.0 (50 mL) and acetone (10 mL) was added papain (500 mg), and the mixture was gently stirred at room temperature for 3 days. The progress of the reaction was monitored by HPLC (column: CHIRALCEL OD-H, Diacel; eluent: petroleum ether/2-propanol 95:5; flow rate: 1.0 mL/min; $\lambda = 254$ nm). When the enzymatic hydrolysis reached 50% conversion, solid $NaHCO_3$ was added, reaction mixture was extracted with diethyl ether, and the pooled organic layers were evaporated to recover the residual ester (+)-**7** (445 mg). The aqueous phase was made acidic with 2 N HCl, and the monoacid (−)-**9** (400 mg) was obtained after extraction with diethyl ether, drying over anhydrous Na_2SO_4, and evaporation of the solvent.

Ethyl (5*R*,2′*R*)-5-(2-*tert*-Butoxycarbonylamino-2-methoxycarbonylethyl)-4,5-dihydroisoxazole-3-carboxylate (+)-7: $[\alpha]^{20}_D$: +79.0 (*c* 1.0, chloroform); colorless oil; Anal. ($C_{15}H_{24}N_2O_7$) C, H, N. Spectroscopic data agreed with those reported for the corresponding racemate.[16]

Ethyl (5*S*,2′*S*)-5-(2-*tert*-Butoxycarbonylamino-2-carboxyethyl)-4,5-dihydroisoxazole-3-carboxylate (−)-9: $[\alpha]^{20}_D$: −171 (*c* 0.1, methanol); colorless oil; R_f 0.57 (chloroform/methanol 9:1 + 50 μL acetic acid). HPLC retention time: 37.20 min (column: CHIRALCEL OD-H, Diacel; eluent: petroleum ether/2-propanol 95:5; flow rate: 1.0 mL/min; λ = 254 nm). ^{1}H NMR ($CDCl_3$): 1.22 (t, $J = 7.2$, 3H), 1.43 (s, 9H), 1.92 (m, 2H), 2.22 (m, 1H), 2.93 (m, 1H), 3.34 (m, 1H), 4.08 (q, $J = 7.2$, 3H), 4.30 (m, 1H), 4.92 (m, 1H), 5.12 (bs, 1H); Anal. ($C_{14}H_{22}N_2O_7$) C, H, N.

(5*S*,2′*R*)-5-(2-Amino-2-carboxyethyl)-4,5-dihydroisoxazole-3-carboxylic Acid (−)-4. Step A. Diester (−)-**6** (345 mg, 1.0 mmol) was dissolved in ethanol (3 mL) and treated with 1 N NaOH (3 mL) at room-temperature overnight. The disappearance of the starting material was monitored by TLC (chloroform/methanol 7:3 + 100 μL acetic acid). The aqueous layer was washed with dichloromethane, made acidic with 2 N HCl, and extracted with ethyl acetate. The organic phase was dried over anhydrous Na_2SO_4, and after evaporation of the solvent, crude (5*S*,2′*R*)-5-(2-*tert*-butoxycarbonylamino-2-carboxy)-4,5-dihydroisoxazole-3-carboxylic acid was obtained as a white powder (220 mg, 0.73 mmol, yield 73%).

Step B. The crude material, obtained from the previous transformation (220 mg, 0.73 mmol), was treated with a 30% dichloromethane solution of trifluoroacetic acid (562 μL, 7.3 mmol) at 0 °C. The solution was stirred at room temperature for 3 h until disappearance of the starting material (TLC: *n*-butanol/water/acetic acid 4:2:1). The volatiles were removed under vacuum, and the residue was washed with methanol and diethyl ether to give (−)-**4**: white prisms; decomposes in the range 175−182 °C. $[\alpha]^{20}_D$: −178.0 (*c* 0.1, water/methanol 1:1). R_f 0.37 (*n*-butanol/water/acetic acid 4:2:1). HPLC retention time: 28.15 min (column: CHIROBIOTIC TAG, Astec; eluant: [ethanol/methanol 3:2]/water 4:1 + 50 mM ammonium acetate + 0.1% acetic acid; flow rate: 1 mL/min; light scattering detection); ee ≥ 99%; Anal. ($C_7H_{10}N_2O_5$) C, H, N. Spectroscopic data agreed with those reported for the corresponding racemate.[16]

(5*R*,2′*S*)-5-(2-Amino-2-carboxyethyl)-4,5-dihydroisoxazole-3-carboxylic Acid (+)-4. Monoacid (+)-**8** (315 mg, 0.95 mmol) was transformed into final amino acid (+)-**4** (overall yield: 60%) following the procedure described above for compound (−)-**4**. (+)-**4**: white prisms; decomposes in the range 155−170 °C; $[\alpha]^{20}_D$: +176.8 (*c* 0.1, water/methanol 1:1); HPLC retention time: 13.75 min (column: CHIROBIOTIC TAG, Astec; eluent: [ethanol/methanol 3:2]/water 4:1 + 50 mM ammonium acetate + 0.1% acetic acid; flow rate: 1 mL/min; light scattering detection); ee ≥ 99%; Anal. ($C_7H_{10}N_2O_5$) C, H, N. Spectroscopic data agreed with those reported for the corresponding racemate.[16]

(5*S*,2′*S*)-5-(2-Amino-2-carboxyethyl)-4,5-dihydroisoxazole-3-carboxylic Acid (−)-5. Monoacid (−)-**9** (400 mg, 1.21 mmol) was transformed into final amino acid (−)-**5** (overall yield: 85%) following the procedure described above for compound (−)-**4**. (−)-**5**: white prisms; decomposes in the range 155−158 °C. $[\alpha]^{20}_D$: −69.0 (*c* 0.1, water/methanol 1:1); HPLC retention time: 10.47 min (column: CHIROBIOTIC TAG, Astec; eluent: [ethanol/methanol 3:2]/water 4:1 + 50 mM ammonium acetate + 0.1% acetic acid; flow rate: 1 mL/min; light scattering detection); ee ≥ 99%; Anal. ($C_7H_{10}N_2O_5$) C, H, N. Spectroscopic data agreed with those reported for the corresponding racemate.[16]

(5*R*,2′*R*)-5-(2-Amino-2-carboxy-ethyl)-4,5-dihydro-isoxazole-3-carboxylic Acid (+)-5. Diester (+)-**7** (445 mg, 1.29 mmol) was transformed into final amino acid (+)-**5** (overall yield: 94%) following the procedure described above for compound (−)-**4**. (+)-**5**: white prisms; decomposes in the range 155−158 °C. $[\alpha]^{20}_D$: +68.0 (*c* 0.1, water/methanol 1:1); HPLC retention time: 19.00 min (column: CHIROBIOTIC TAG, Astec; eluent: [ethanol/methanol 3:2]/water 4:1 + 50 mM ammonium acetate + 0.1% acetic acid; flow rate: 1 mL/min; light scattering detection); ee ≥ 99%; Anal. ($C_7H_{10}N_2O_5$) C, H, N. Spectroscopic data agreed with those reported for the corresponding racemate.[16]

Methyl (*S*)-(+)-2-*tert*-Butoxycarbonylamino-4-pentenoate (+)-10. Dipolarophile (+)-**10** was prepared from commercially available (*S*)-(−)-2-amino-4-pentenoic acid following a literature procedure.[20]

(5*R*,2′*S*)-5-(2-*tert*-Butoxycarbonylamino-2-methoxycarbonylethyl)-4,5-dihydroisoxazole-3-carboxylic Acid Ethyl Ester (+)-6 and (5*S*,2′*S*)-5-(2-*tert*-Butoxycarbonylamino-2-methoxycarbonylethyl)-4,5-dihydroisoxazole-3-carboxylic Acid Ethyl Ester (−)-7. To a solution of (+)-**10** (710 mg, 3.10 mmol) in ethyl acetate (10 mL) was added ethyl 2-chloro-2-(hydroxyimino)acetate (705 mg, 4.65 mmol) and sodium bicarbonate (1 g). The mixture was vigorously stirred for 3 days at room temperature; the progress of the reaction was monitored by TLC (petroleum ether/ethyl acetate 7:3). Water was added to the reaction mixture and the organic layer was separated and dried over anhydrous Na_2SO_4. The crude material, obtained after evaporation of the solvent, was chromatographed on silica gel (petroleum ether/ ethyl acetate 4:1) to give 350 mg of (+)-**6** and 556 mg of (−)-**7**. Overall yield 85%. (+)-**6**: $[\alpha]^{20}_D$: +70.6 (*c* 1.0, chloroform). Anal. ($C_{15}H_{24}N_2O_7$) C, H, N. Spectroscopic data agreed with those reported for the corresponding racemate.[16] (−)-**7:** $[\alpha]^{20}_D$: −78.2 (*c* 1.0, chloroform). Anal. ($C_{15}H_{24}N_2O_7$) C, H, N. Spectroscopic data agreed with those reported for the corresponding racemate.[16]

Receptor Binding at iGluRs. The membrane preparations used in receptor-binding experiments were prepared according to Ransom and Stec[35] with slight modifications, as previously described.[26] Affinity for AMPA,[23] KA,[24] and NMDA[22] receptor sites was determined using 5 nM [^{3}H]AMPA, 5 nM [^{3}H]KA in the absence of $CaCl_2$, and 2 nM [^{3}H]CGP 39653 ([^{3}H]-(±)-(*E*)-2-amino-4-propyl-5-phosphono-3-pentenoate), respectively. The tritiated ligands were all purchased from New England Nuclear (NEN). The amount of bound radioactivity was determined using a Packard TOP-COUNT microplate scintillation counter. Binding data were analyzed by nonlinear regression using GraphPad Prism 3.03 (GraphPad Software, San Diego, CA). Data were fitted to the following equation: $B = B_{max} - (B_{max} \times [\text{inhibition}]^n)/(IC_{50}^n + [\text{inhibitor}]^n)$, where B is the binding, expressed as a percentage of total specific binding, and n is the Hill coefficient.

Electrophysiology of NMDA Receptors in *Xenopus* Oocytes. For expression in *Xenopus* oocytes, rat NR1-1a, NR2A, NR2B, NR2C, and NR2D were subcloned into pCI-neo containing a T7 site upstream from the 5′ untranslated region (UTR). Linearized plasmids were used to produce NR1-1a, NR2A, NR2B, NR2C, and NR2D cRNAs with mMessage mMachine kits (Ambion). Oocytes were surgically removed from mature female *Xenopus laevis* anaesthetized in a 0.4% MS-222 (3-aminobenzoic acid ethyl ester, Sigma) solution for 10−15 min. To remove the follicle layer, the oocytes were subsequently digested with 0.5 mg/mL collagenase (type IA, Sigma) in OR-2 buffer (in mM: 82.5 NaCl, 2.0 KCl, 1.0 $MgCl_2$, and 5.0 HEPES pH 7.6) at room temperature for 2−3 h. Healthy-looking stage V−VI oocytes were selected for injection the following day. Oocytes were coinjected with cRNA encoding NR1-1a and either of the NR2 subunits at a 1:1 ratio,

respectively, and maintained in Barth's solution (in mM: 88 NaCl, 1.0 KCl, 2.4 $NaHCO_3$, 0.41 $CaCl_2$, 0.82 $MgSO_4$, 0.3 $Ca(NO_3)_2$, 15 HEPES pH 7.5, 100 IU/mL penicillin, and 100 μg/mL streptomycin) at 18 °C. Recordings were performed 2−4 days after injection using whole-cell two-electrode voltage-clamp at −40 mV to −100 mV in Ca^{2+}- and Mg^{2+}-free Ringers solution containing (in mM) 115 NaCl, 2.5 KCl, 1.9 $BaCl_2$, and 10 HEPES (pH 7.6). During recording, 10 μM glycine was included in all agonist and/or antagonist applications. Single concentration tests were performed in at least triplicates with two independent experiments. Electrophysiological data were acquired using Clampex 7.0 (Axon Instruments) and subsequently processed with GraphPad Prism 4.0 (GraphPad Software, San Diego, CA).

Metabotropic Testing. The mGluR subtypes mGluR1a, mGluR2 and mGluR4a were stably expressed in Chinese hamster ovary (CHO) cell lines. Cells were maintained and tested as previously described by measurement of intracellular calcium (mGluR1) or cyclic AMP (mGluR2,4) levels.[25]

Oxygen−Glucose Deprivation in Cortical Cell Cultures. Cultures of mixed cortical cells containing both neuronal and glial elements were prepared, used at 14 days in vitro, and exposed to OGD as previously described.[27] Briefly, culture medium was replaced by a glucose-free balanced salt solution saturated with 95% N_2/5% CO_2 and heated to 37 °C. Multiwells were then sealed into an airtight incubation chamber equipped with inlet and outlet valves and 95% N_2/5% CO_2 was blown through the chamber for 10 min to ensure maximal removal of oxygen. The chamber was then sealed and placed into the incubator at 37 °C for 60 min. OGD was terminated by removing the cultures from the chamber, replacing the exposure solution with oxygenated medium, and returning the multiwells to the incubator under normoxic conditions. The extent of neuronal death was assessed 24 h later. In this system, 60 min OGD induced a neuronal damage that was approximately 75% of the maximal degree of neuronal injury achieved by exposing the cultures for 24 h to 1 mM glutamate. OGD-induced cell injury was quantitatively evaluated by measuring the amount of LDH released from injured cells into culture media 24 h following exposure to OGD, as previously described.[27] The LDH level corresponding to complete neuronal death (with no glial death) was determined for each experiment by assaying sister cultures exposed to 1 mM glutamate for 24 h. Background LDH release was determined in control cultures not exposed to OGD and subtracted from all experimental values. The resulting value correlated linearly with the degree of cell loss estimated by observation of cultures under phase-contrast microscopy or under bright-field optics following 5 min incubation with 0.4% trypan blue, which stains debris and nonviable cells.

Molecular Modeling of NMDA Receptor Antagonists. *Ligand Geometry and Conformation*. All ligands, built using Sybyl6.8,[36] were preliminarily minimized by conjugated gradient utilizing the Tripos force field.[36] The amino, carboxyl, and phosphonate groups were ionized to better simulate the physiological conditions. The charges were assigned by MOPAC/PM3 calculation implemented in SYBYL environment.

Dockings. The open form of the NMDA/NR2A homology model described by Grazioso et al.[17] was chosen for the flexible docking calculations. We used the putative binding site of the NR2A protein surrounding the amino acids that have been described as essential for l-Glu and (*R*)-AP5 binding.[28,29] GOLD 2.1,[37,38] used for the molecular docking calculations, employs a genetic algorithm (GA) wherein the molecular features of the protein−ligand complexes are encoded as a chromosome. The protein required for the calculations was considered with all hydrogen atoms, and the implemented algorithm successively optimized the orientation of the hydroxyl hydrogen atom of residues Tyr, Thr, Ser, and Lys located into the binding pocket. Lone pairs were automatically added with the default geometry; the cavity was detected with an active site radius of 12.0 Å from the side chain hydrogen atom of residue T513. The Goldscore fitness function and the torsion angle distributions were chosen to improve the quality of the docking results. van der Waals and hydrogen bonding radii were set to 4.0 and 3.0 Å, respectively; the genetic algorithm parameters were kept at the default value. Finally, the obtained docking results were visually analyzed by Sybyl 6.8, to evaluate both the quality and the accordance of the resulting binding mode with the experimental data.

Molecular Modeling of mGluR2 Receptor Agonists. *Pharmacophore Models*. The conformational flexibility of each molecule was investigated through a stimulated annealing protocol as described by N. Jullian[31] using the Discover calculation engine with the CFF91 force field (Insight II version 2001, Accelrys San Diego). It appears that the two isomers (−)-**2** and (+)-**3** adopt only one stable conformation. We superimposed them to the model by using the three functional groups as anchor points (distal and proximal carboxylate carbon atoms, amino group nitrogen atom) (Insight II, Accelrys San Diego).

Dockings. Each stereoisomer was docked at the Glu binding site of mGlu2R ATD model described by Bertrand et al.[18] The ligands were first manually positioned by superimposing the α-carboxylate, the amino group, and the γ-carboxylate on those of Glu. The obtained protein−ligand complex was therefore subjected to energy minimization (steepest-descent convergence, 10 kcal. $mol^{-1}\cdot Å^{-1}$; conjugate-gradient convergence, 0.1 kcal. $mol^{-1}.Å^{-1}$) while fixing with a restraint between 100 and 1000, the following distances: oxygen of the α-carboxylate of ligand−S123 oxygen at 2.65 Å; ligand's nitrogen−A144 oxygen of the carbonyl at 2.8 Å; ligand's nitrogen−T146 oxygen at 2.95 Å. These calculations were performed as previously described using the Discover 3.00 calculation engine with the CFF force field (Insight II version 2001, Accelrys, San Diego).[18]

Acknowledgment. Professor Shigetada Nakanishi is gratefully acknowledged for the kind gift of the mGluR-expressing CHO cell lines. This work was financially supported by MIUR (COFIN 2003) Rome and Università degli Studi di Milano (FIRST). G.G. wishes to thank Professor Leonardo Scapozza (Laboratoire de Chimie Thérapeutique, Section des Sciences Pharmaceutiques, Université de Genéve, Switzerland.) for his kind support in the utilization of the GOLD modeling software. H.B.O. was supported by the Danish Medical Research Council and the Novo Nordisk Foundation. FA wishes to thank Dr H.-O. Bertrand (Accelerys, Orsay France) for his constant and valuable support as well as the C.N.R.S, the French ministry of reseach, RETINA-France, and the Fondation de France for funding.

Supporting Information Available: Elemental analyses. This material is available free of charge via the Internet at http://pubs.acs.org.

References

(1) Wheal, H. V., Thomson, A. M., Eds. *Excitatory Amino Acids and Synaptic Transmissions*; Academic Press: London, 1995.
(2) Bräuner-Osborne, H.; Egebjerg, J.; Nielsen, E. Ø.; Madsen, U.; Krogsgaard-Larsen, P. Ligands for glutamate receptors: Design and therapeutic prospects. *J. Med. Chem*. **2000**, *43*, 2609−2645.
(3) Dingledine, R.; Borges, K.; Bowie, D.; Traynelis, S. F. The glutamate receptor ion channels. *Pharmacol. Rev.* **1999**, *51*, 7−61.
(4) Pin, J.-P.; Acher, F. The metabotropic glutamate receptors: structure, activation mechanism and pharmacology. *Curr. Drug Targets − CNS & Neurol. Dis.* **2002**, *1*, 297−317.
(5) Cull-Candy, S.; Brickley, S.; Farrant, M. NMDA receptor subunits: diversity, development and disease. *Curr. Opin. Neurobiol.* **2001**, *11*, 327−335.
(6) Schorge, S.; Colquhoun, D. Studies of NMDA receptor function and stoichiometry with truncated and tandem subunits. *J. Neurosci.* **2003**, *23*, 1151−1158.
(7) Das, S.; Sasaki, Y. F.; Rothe, T.; Premkumar, L. S.; Takasu, M.; Crandall, J. E.; Dikkes, P.; Conner, D. A.; Rayudu, P. V.; Cheung, W.; Chen, H. S. V.; Lipton, S. A.; Nakanishi, N. Increased NMDA current and spine density in mice lacking the NMDA receptor subunit NR3A. *Nature (London)* **1998**, *393*, 377−381.

(8) Chatterton, J. E.; Awobuluyl, M.; Premkumar, L. S.; Takanishi, H.; Talantova, M.; Shin, Y.; Cui, J.; Tu, S.; Sevarino, K. A.; Nakanishi, N.; Tong, G.; Lipton, S. A.; Zhang, D. Excitatory glycine receptors containing the NR3 family of NMDA receptor subunits. *Nature (London)* **2002**, *415*, 793−798.
(9) Kemp, J. A.; Kew, J. N. C.; Gill, R. *Handbook of Experimental Pharmacology*; Jonas, P., Monyer, H., Eds.; Springer: Berlin, 1999; Vol. 141, pp 495−527.
(10) Lees, K. R.; Asplund, K.; Carolei, A.; Davis, S. M.; Diener, H. C.; Kaste, M.; Orgogozo, J. M.; Whitehead, J. Glycine antagonist (gavestinel) in neuroprotection (GAIN International) in patients with acute stroke: a randomised controlled trial. GAIN International Investigators. *Lancet* **2000**, *355*, 1949−1954.
(11) Nikam, S. S.; Meltzer, L. T. NR2B Selective NMDA Receptor Antagonists. *Curr. Pharm. Des*. **2002**, *8*, 845−855.
(12) Gotti, B.; Duverger, D.; Bertin, J.; Carter, C.; Dupont, R.; Frost, J.; Gaudilliere, B.; MacKenzie, E. T.; Rousseau, J.; Scatton, B. Ifenprodil and SL 82.0715 as cerebral anti-ischemic agents. I. Evidence for efficacy in models of focal cerebral ischemia. *J. Pharmacol. Exp. Ther.* **1988**, *247*, 1211−1221.
(13) Kemp, J. A.; McKerman, R. M. NMDA receptor pathways as drug targets. *Nature Neurosci.* **2002**, *5*, 1039−1042.
(14) Conti, P.; De Amici, M.; Joppolo di Ventimiglia, S.; Stensbøl, T. B.; Madsen, U.; Bräuner-Osborne, H.; Russo, E.; De Sarro, G.; Bruno, G.; De Micheli, C. Synthesis and anticonvulsant activity of novel bicyclic acidic amino acids. *J. Med. Chem.* **2003**, *46,* 3102−3108.
(15) Roda, G.; Conti, P.; De Amici, M.; He, J.; Polavarapu, P. L.; De Micheli, C. Enantiopure stereoisomeric homologues of glutamic acid: chemoenzymatic synthesis and assignment of their absolute configuration. *Tetrahedron: Asymmetry* **2004**, *15*, 3079−3090.
(16) Conti, P.; De Amici, M.; Grazioso, G.; Roda, G.; Barberis Negra, F.; Nielsen, B.; Stensbøl, T. B.; Madsen, U.; Bräuner-Osborne, H.; Frydenvang, K.; De Sarro, G.; Toma, L.; De Micheli, C. Design, synthesis and pharmacological characterization of novel potent NMDA receptor antagonists. *J. Med. Chem*. **2004**, *47*, 6740−6748.
(17) Grazioso G.; Moretti, L.; Scapozza, L.; De Amici, M.; De Micheli, C. Development of a threee-dimensional model for the *N*-Methyl-d-Aspartate NR2A subunit. *J. Med. Chem*. **2005**, *48*, 5489−5494.
(18) Bertrand, H.-O.; Bessis; A.-S.; Pin, J.-P.; Acher, F. Common and selective molecular determinants involved in metabotropic glutamate receptor agonist activity. *J. Med. Chem*. **2002**, *45*, 3171−3183.
(19) Sih, C. J.; Wu, S.-H. In *Topics in Stereochemistry*; Eliel, E. L.; Wilen, S. H.; Eds.; John Wiley & Sons: New York, 1989; Vol. 19, pp 63−125.
(20) Collier, P. N.; Campbell, A. D.; Patel, I.; Taylor, R. J. K. The direct synthesis of novel enantiomerically pure α-amino acids in protected form via Suzuki cross-coupling. *Tetrahedron Lett*. **2000**, *41*, 7115−7119.
(21) Kozikowski, A. P.; Adamczyk, M. Methods for the stereoselective *cis*-cyanohydroxylation of olefins. *J. Org. Chem.* **1983**, *48*, 366−372.
(22) Sills, M. A.; Fagg, G.; Pozza, M.; Angst, C.; Brundish, D. E.; Hurt, S. D.; Wilusz, E. J.; Williams, M. [3H]CGP 39653: a new *N*-methyl-d-aspartate antagonist radioligand with low nanomolar affinity in rat brain. *Eur. J. Pharmacol.* **1991**, *192*, 19−24.
(23) Honoré, T.; Nielsen, M. Complex structure of quisqualate-sensitive glutamate receptors in rat cortex. *Neurosci. Lett.* **1985**, *54*, 27−32.
(24) Braitman, D. J.; Coyle, J. T. Inhibition of [3H]kainic acid receptor binding by divalent cations correlates with ion affinity for the calcium channel. *Neuropharmacology* **1987**, *26*, 1247−1251.
(25) Bjerrum, E. J.; Kristensen, A. S.; Pickering, D. S.; Greenwood, J. R.; Nielsen, B.; Liljefors, T.; Schousboe, A.; Bräuner-Osborne, H.; Madsen, U. Design, synthesis, and pharmacology of a highly subtype-selective GluR1/2 agonist, (*RS*)-2-amino-3-(4-chloro-3-hydroxy-5-isoxazolyl)propionic acid (Cl-HIBO). *J. Med. Chem.* **2003**, *46*, 2246−2249.
(26) Clausen, R. P.; Hansen, K. B.; Cali, P.; Nielsen, B.; Greenwood, J. R.; Begtrup, M.; Egebjerg, J.; Brauner-Osborne, H. The respective *N*-hydroxypyrazole analogues of the classical glutamate receptor ligands ibotenic acid and (*R*,*S*)-2-amino-2-(3-hydroxy-5-methyl-4-isoxazolyl)acetic acid. *Eur. J. Pharmacol.* **2004**, *499*, 35−44.
(27) For details see: Pellegrini-Giampietro, D. E.; Cozzi, A.; Leonardi, P.; Peruginelli, F.; Meli, E.; Pellicciari, R.; Moroni, F. 1-Amino-1,5-dicarboxylic acid and (*S*)-(+)-2-(3′-carboxybicyclo[1.1.1]pentyl)-glycine, two mGlu1 receptor-preferring antagonists, reduce neuronal death in *in vitro* and *in vivo* models of cerebral ischemia. *Eur. J. Neurosci.* **1999**, *11*, 3637−3647.
(28) Anson, L. C.; Chen, P. E.; Wyllie, D. J. A.; Colquhoun, D.; Schoepfer, R. Identification of amino acid residues of the NR2A subunit that control glutamate potency in recombinant NR1/NR2A NMDA receptors. *J. Neurosci.* **1998**, *18*, 581−589.
(29) Lummis, S. C. R.; Fletcher, E. J.; Green, T. Identification of a new site in the S1 ligand binding region of the NMDA receptor NR2A subunit involved in receptor activation by glutamate. *Neuropharmacology* **2002**, *42*, 437−443.
(30) Branden, C.; Tooze, J. *Introduction to protein structure*, 2nd ed.; Garland Ed. Publishing: New York, 1999; pp16−18.
(31) Jullian, N.; Brabet, I.; Pin, J.-P.; Acher, F. Agonist selectivity of mGluR1 and mGluR2 metabotropic receptors: a different environment but similar recognition of an extended glutamate conformation. *J. Med. Chem.* **1999**, 42, 1546−1555.
(32) Kunishima, N.; Shimada, Y.; Tsuji, Y.; Sato, T.; Yamamoto, M.; Kumasaka, T.; Nakanishi, S.; Jingami, H.; Morikawa, K. Structural basis of glutamate recognition by a dimeric metabotropic glutamate receptor. *Nature (London)* **2000**, *407*, 971−977.
(33) Acher, F.; Bertrand, H.-O. Amino acid recognition by Venus Flytrap domains is encoded in an 8 residue motif. *Biopolymers* **2005**, *80*, 357−366.
(34) Bessis, A.-S.; Rondard, P.; Gaven, F.; Brabet, I.; Triballeau, N.; Prézeau, L.; Acher, F.; Pin, J.-P. Closure of the Venus flytrap module of mGlu8 receptor and the activation process: insights from mutations converting antagonists into agonists. *Proc. Natl. Acad. Sci. U.S.A.* **2002**, *99*, 11097−11102.
(35) Ransom, R. W.; Stec, N. L. Cooperative modulation of [3H]MK-801 binding to the *N*-methyl-d-aspartate receptor-ion channel complex by l-glutamate, glycine and polyamines. *J. Neurochem.* **1988**, *51*, 830−836.
(36) *Sybyl 6.8*, Tripos Inc., 1699 South Hanley Rd., St. Louis, MO 63144.
(37) *GOLD v. 2.1*, Cambridge Crystallographic Data Centre: Cambridge, U.K.
(38) Verdonk, M. L.; Cole, J. C.; Hartshorn, M. J.; Murray, C. W.; Taylor, R. D. Improved Protein−Ligand Docking Using GOLD. *Proteins* **2003**, *52*, 609−623. Available: http://www.ccdc.cam.ac.uk

JM0504499